

引用格式: PENG Jiali, RUAN Ping, XIE Youjin, et al. Dynamic Characteristics Analysis of Space Electro-optical Tracking and Pointing Turntable[J]. Acta Photonica Sinica, 2023, 52(7):0712002

彭加力,阮萍,谢友金,等. 星载光电跟瞄转台动态特性分析[J]. 光子学报, 2023, 52(7):0712002

星载光电跟瞄转台动态特性分析

彭加力^{1,2,3}, 阮萍^{1,3}, 谢友金^{1,3}, 李治国^{1,3}, 王佳浩^{1,2,3}, 韩璟宇^{1,2,3}

(1 中国科学院西安光学精密机械研究所, 西安 710119)

(2 中国科学院大学, 北京 100049)

(3 中国科学院空间精密测量技术重点实验室, 西安 710119)

摘要: 针对目前利用有限元方法分析星载光电跟瞄转台动态特性时存在的建模失真问题, 提出使用广义弹簧单元对轴承和锁紧机构等效建模, 并通过定义模态阻尼比, 精确模拟转台的固有频率及响应特性。通过理论计算和基于模态试验数据的参数辨识, 确定各等效单元刚度; 通过基于扫频试验数据的参数辨识, 确定结构模态阻尼。基于建立的等效有限元模型进行仿真分析, 模态分析中前 6 阶固有频率与试验结果的最大偏差为 5.1%, 谐响应分析中 X、Y、Z 三个主方向的最大响应与试验结果的最大偏差为 3.2%, 固有频率与响应一致性良好, 均在允许的误差范围内。说明使用广义弹簧单元对轴承和锁紧机构进行等效建模, 通过模态和扫频试验数据确定转台刚度和阻尼特性是可行的, 对同类型转台的建模仿真有一定借鉴作用。

关键词: 精密仪器与机械; 动态特性; 等效建模; 星载光电跟瞄转台; 刚度与阻尼; 固有频率; 振动响应; 有限元分析

中图分类号: TH123

文献标识码: A

doi: 10.3788/gzxb20235207.0712002

0 引言

星载光电跟瞄转台是一种空间光电载荷, 用以在干扰因素复杂的空间环境中实现系统光轴的稳定及对目标的跟踪, 广泛应用于空间观测和激光通信等领域, 是光电测控领域的重要单机装备^[1-5], 美国天基空间目标监视(Space-Based Space Surveillance, SBSS)系统, 日本(Optical Inter-orbit Communications Engineering Test Satellite, OICETS)卫星上搭载的(Laser Utilizing Communication Equipment, LUCE)激光通信终端以及我国探月工程中的极紫外相机(Extreme Ultraviolet Camera, EUVC)等均使用了星载光电跟瞄转台^[6-9]。

在发射过程中, 星载光电跟瞄转台受运载火箭产生的加速度动载荷作用, 转台及光电载荷将会产生不同程度的振动响应, 响应大小与动载荷量级成正比。当激励频率与系统本身固有频率接近时, 将会产生共振现象, 响应被放大, 由于系统存在一定的阻尼, 响应不会至无穷大, 但过高的响应放大依旧会对光学系统的工作性能、精度、效率、寿命、安全性和可靠性等产生直接影响。因此分析星载光电跟瞄转台的动态特性, 确定系统固有频率及响应, 对光机系统的设计以及环境试验的实施具有重要指导作用。

工程中往往通过有限元方法获取转台动态特性, 因而建立能够准确反映转台刚度和阻尼特性的有限元模型是准确分析固有频率及响应特性的关键。转台刚度特性由材料、构件的截面以及各构件连接处的刚度决定, 对于确定结构来说, 各构件连接部位作为载荷的传递路径, 其刚度特性直接影响着转台整体的刚度特性。国内对于星载光电跟瞄转台动态特性的仿真并不少见, 但对于连接部位(轴承、锁紧机构)的建模容易失真。轴承建模方面, 张永强等^[10]保留轴承实体, 基于 Hertz 接触理论进行了轴承参数化建模, 由于计算规

基金项目: 中国科学院青年创新促进会项目(No. 2018441)

第一作者: 彭加力, pengjiali_echo@163.com

通讯作者: 阮萍, ruanp@opt.ac.cn

收稿日期: 2023-02-08; 录用日期: 2023-03-17

<http://www.photon.ac.cn>

模极大,该方法一般只在专门对轴承进行研究时才会选择;贺帅^[11]利用多点约束单元(Multi Point Constraints, MPC)对二维转台中的轴承进行了刚性等效建模,只保留了轴承绕轴线旋转自由度,其它自由度的刚度无穷大,与实际情况相差较大,只在轴承连接关系对仿真结果影响不大时使用;秦涛等^[12]利用两组一维弹簧单元(Spring)分别模拟轴承径向位移刚度和轴向位移刚度,是目前轴承等效建模的主要方法,这种方法能真实反映轴承的位移刚度,但忽略了轴承的角刚度。锁紧机构建模方面的相关研究较少,陈卓^[13]去除锁紧机构中爆炸螺栓等结构,锁紧支架和支座利用MPC单元刚性等效建模,将连接接合面之间的刚度考虑为无穷大,与实际情况相差较大。上述建模方法虽然能在一定程度上等效轴承和锁紧机构,但均存在诸如收敛难度大、建模复杂或连接刚度过大等问题,不能真实反映系统动态特性。

基于上述原因,本文根据某星载光电跟瞄转台的结构组成,提出一种使用广义弹簧单元对轴承和锁紧机构进行等效建模的方法,通过理论计算以及基于模态和扫频试验数据的参数辨识,确定各连接部位的刚度及结构的模态阻尼,分析星载光电跟瞄转台动态特性。

1 星载光电跟瞄转台建模

1.1 转台结构组成

星载光电跟瞄转台主要包括载物台及光电负载、方位轴、俯仰左轴、俯仰右轴、U型架和锁紧机构等,总体结构如图1所示。

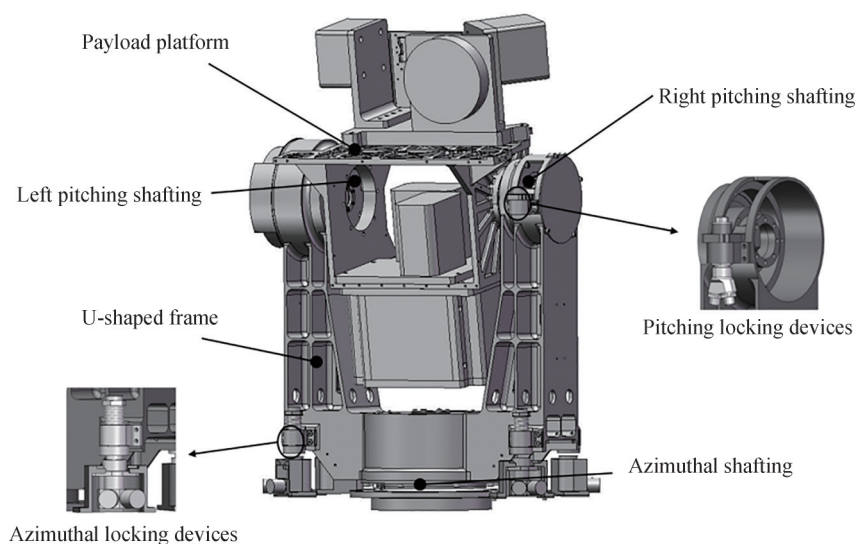


图1 星载光电跟瞄转台总体结构

Fig.1 Overall structure of space electro-optical tracking and pointing turntable

U型架是连接俯仰轴系和方位轴系的主体,既是俯仰轴系的支撑结构,又固连于方位轴系;方位轴系采用一对背靠背安装的角接触球轴承,用于承受各向载荷;俯仰轴系两端轴承采用一端固定一端游动的安装方式,左轴为固定端,选用一对背靠背安装的角接触球轴承;右轴为游动端,选用深沟球轴承,实现温度补偿;光电负载依靠U型架结构来支撑和驱动,实现绕方位轴和俯仰轴的旋转;锁紧机构是星载光电跟瞄转台的重要组成部分,在发射过程中锁紧,抑制轴系旋转并且提供辅助支撑,提高整体刚度,入轨运行后解锁,释放转台转动自由度。

1.2 轴系及锁紧机构等效建模

采用广义弹簧单元(Bushing)对跟瞄转台中的轴承和锁紧机构进行等效建模。Bushing单元又称衬套单元,是一种三向弹簧-阻尼单元,常用于绳索和柔节等多自由度结构的建模^[14-16],至多具有6个自由度,包括3个主方向的平动和转动,如图2所示。

Bushing单元提供一个6阶刚度矩阵,通过调整刚度矩阵中的参数,可以起到抑制或释放对应自由度运动的作用,模拟单元内部的刚度分布,其刚度矩阵表述为

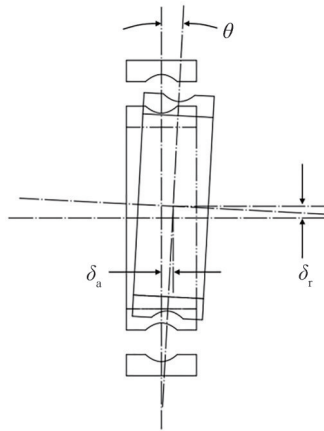


图4 径向、轴向和力矩载荷联合作用下轴承相对位移

Fig.4 Relative displacement of inner-outer rings under the combined action of radial, axial and moment loads

1.2.2 锁紧机构等效建模

锁紧机构由锁紧支架、锁紧支座以及火工螺栓组成。其结构与普通螺栓类似,火工螺栓贯穿锁紧支架和支座,在预紧力作用下形成一对结合面。动载荷作用时,结合面间存在法向接触力 F_N 和切向摩擦力 F_T ,各方向有滑移、分离、翻转等趋势^[19],如图5所示。

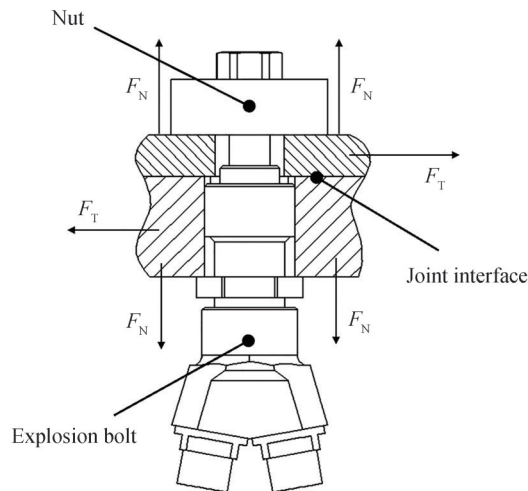


图5 锁紧机构力学模型

Fig.5 Mechanical model of the locking devices

假设爆炸螺栓轴向为 Z ,则在锁紧机构刚度矩阵式(2)中, k_x 、 k_y 和 k_z 分别代表锁紧机构三个主方向的位移刚度,表征动载荷作用下结合面间各方向的分离趋势; k_{θ_x} 、 k_{θ_y} 和 k_{θ_z} 分别代表锁紧机构三个主方向的角刚度,表征动载荷作用下结合面绕各方向的翻转趋势。

简化轴系,去除电机、谐波减速器等构件,只保留主轴和U型架,分别建立方位轴、俯仰左轴及俯仰右轴共3个Bushing单元,简化建模过程中导致的质量缺失,通过0维质量单元(Point Mass)补足,如图6所示。

简化锁紧机构,去除火工螺栓,只保留锁紧支架和支座,分别建立俯仰锁紧机构及4个方位锁紧机构共5个Bushing单元,如图7所示。

简化其它结构,去除不必要的构件以及倒圆角、孔等特征。除轴承和锁紧机构外,其它各构件连接处均使用刚性连接处理。方位轴座和方位锁紧支座底部约束,最终建立的有限元模型质量为49.5 kg,接近真实质量。节点数为98万,网格数为64万,有限元模型如图8所示。

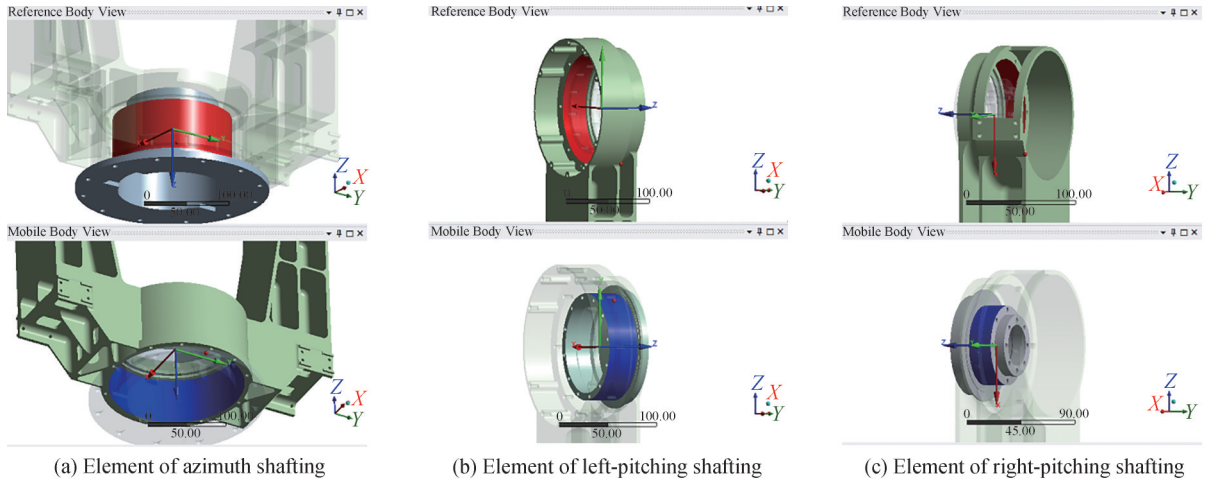


图6 轴系 Bushing 单元
Fig.6 Bushing element of shafting

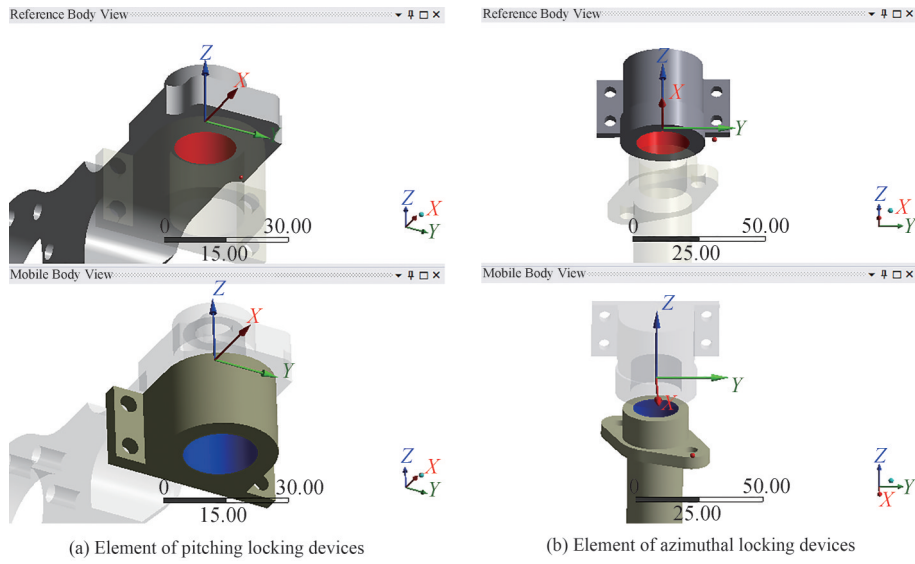


图7 锁紧机构 Bushing 单元
Fig.7 Bushing element of locking devices

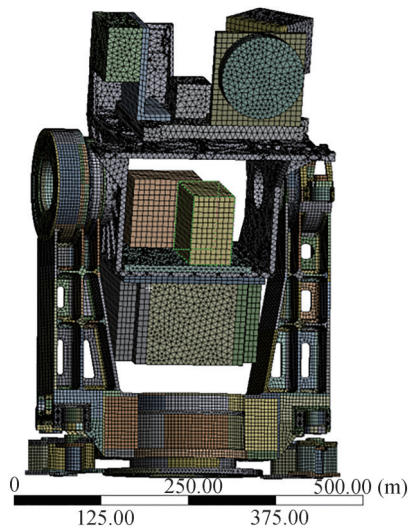


图8 星载光电跟踪转台有限元模型示意图
Fig.8 Finite element model of space electro-optical tracking and pointing turntable

2 跟瞄转台刚度特性分析

通过轴承刚度理论计算和基于多工况模态试验数据的参数辨识,获取各 Bushing 单元的刚度矩阵。

2.1 轴承刚度理论计算

方位轴和俯仰左轴的角接触球轴承,通过预紧消除游隙,提高轴系的刚度以及旋转。角接触球轴承同时承受径向载荷和轴向载荷,对轴承进行受力平衡分析,得到预紧力作用下的角接触球轴承的位移刚度为^[10,20]

$$k_{x,y} = 1704D_w^{1/3} Z^{2/3} \frac{\cos^2 \alpha}{\sin^{1/3} \alpha} F_a^{1/3} \quad (3)$$

$$k_z = 3409D_w^{1/3} Z^{2/3} \sin^{5/3} \alpha F_a^{1/3} \quad (4)$$

式中, $k_{x,y}$ 为径向刚度, k_z 为轴向刚度, D_w 为滚子直径, Z 为滚子数, α 为接触角, F_a 为轴向预紧力。

由于左右轴承间支承跨距较大,俯仰左轴角接触球轴承具有一定径向角刚度,根据右轴径向位移刚度推导得出

$$k_{\theta_x, \theta_y} = k_r l / \arctan(1/l) \quad (5)$$

式中, k_{θ_x, θ_y} 为左轴径向角刚度; k_r 为右轴径向位移刚度; l 为俯仰轴系支承跨距。

右轴的深沟球轴承径向悬空布置,其静刚度为0,但在承受动载荷时,轴承外圈与负载压紧,轴承实际具有一定动刚度。这种动载荷下深沟球轴承的刚度特性目前尚未有文献进行深入探讨,往往通过工程经验给出刚度值。

通过理论计算并结合工程经验,给出轴承刚度部分参数如表1,其余难以理论计算的刚度参数利用多工况的模态试验数据,进行模型参数辨识得出。

表1 轴承刚度矩阵计算值
Table 1 Bearing stiffness calculation results

	$k_{x,y} / (\text{N} \cdot \text{mm}^{-1})$	$k_z / (\text{N} \cdot \text{mm}^{-1})$	$k_{\theta_x, \theta_y} / (\text{N} \cdot \text{mm}/^\circ)$	$k_{\theta_z} / (\text{N} \cdot \text{mm}/^\circ)$
Azimuth shafting	2.5×10^5	1.1×10^5	—	—
Left-pitching shafting	1.6×10^5	70 000	5.1×10^7	—
Right-pitching shafting	30 000	300	0	0

2.2 模态试验设计

模态试验采用德国 M+P International 公司的 32 通道数据采集系统和 Smart Office Analyzer 数据处理分析软件进行,试验现场如图 9 所示。试验采用锤击法,按结构划分测点,使用 10 个量程为 50 g (g 为重力加速度)的加速度传感器,分 4 个批次采集结构上选定的 40 个测点的振动响应信号。

模态试验前 6 阶固有频率及振型描述如表 2,振型如图 10 所示。

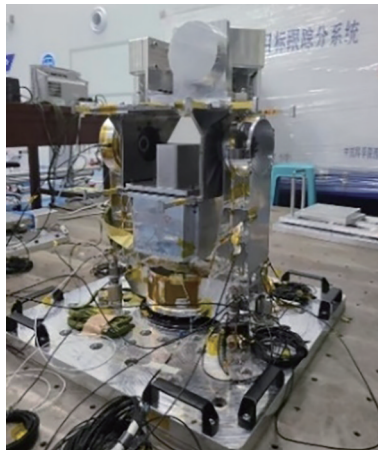


图9 星载光电跟瞄转台模态试验

Fig.9 Modal test of space electro-optical tracking and pointing turntable

表 2 模态试验前 6 阶固有频率
Table 2 The first six natural frequencies of modal test

Mode	Nature frequency/Hz	Modal shape
1	44.1	Rotate around pitching shafting
2	66.5	Swing back and forth
3	67.4	Swing left and right
4	106.7	Rotate around azimuth shafting
5	174.8	Local modal
6	186.5	Swing up and down

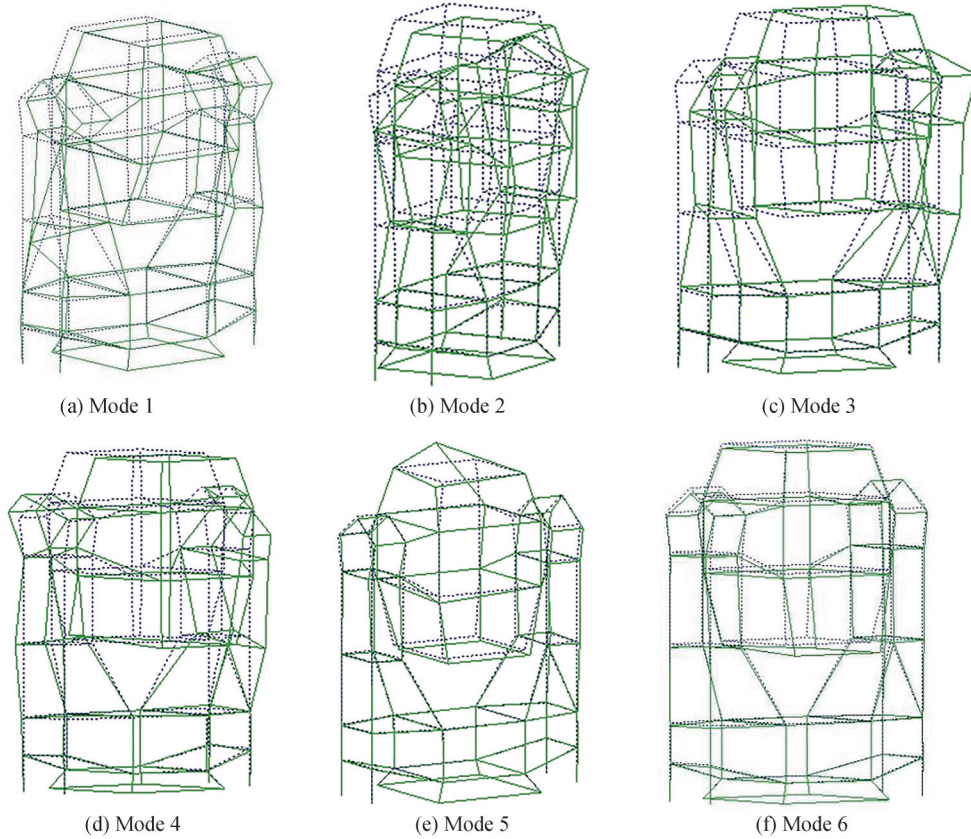


图 10 模态试验前 6 阶振型图
Fig. 10 The first six mode shapes of modal test

为单独分析各锁紧机构及轴系对整体刚度的影响,根据锁紧机构的不同状态,设置表 3 所示 3 种试验工况。通过将各振型的仿真固有频率与试验固有频率匹配,得出影响各阶振型的刚度参数。

表 3 模态试验工况
Table 3 Modal test setting

No.	Working conditions	
	Azimuth locking devices	Pitching locking devices
1	Unlocked	Unlocked
2	Unlocked	Locked
3	Locked	Locked

2.3 基于模态试验数据的刚度参数辨识

2.3.1 俯仰轴系刚度辨识

工况1中俯仰锁紧机构解锁,光电负载绕俯仰轴旋转只由俯仰谐波的角刚度决定。即俯仰左轴刚度参数 k_{θ_z} 决定光电负载绕俯仰轴旋转阶振型固有频率,根据工况1试验结果,试算确定 $k_{\theta_z}=4\times 10^5\text{ N}\cdot\text{mm}/^\circ$,试验与仿真结果如表4。

表4 俯仰轴系刚度辨识
Table 4 Stiffness identification of pitching shafting

Mode shape	Rotate around pitching shafting
Working conditions	1
Test/Hz	32.7
Simulation/Hz	33.5
Relative error/%	2.4

2.3.2 方位轴系刚度辨识

工况1中方位锁紧机构解锁,转台只靠方位轴系支撑,转台的左右摆动、前后摆动以及绕方位轴旋转均由方位轴系的角刚度决定。即方位轴系刚度参数 k_{θ_x} 决定转台左右摆动阶振型固有频率; k_{θ_y} 决定转台前后摆动阶振型固有频率;方位谐波角刚度 k_{θ_z} 决定转台绕方位轴扭转阶振型固有频率。根据工况1试验结果,试算确定 $k_{\theta_x}=2.5\times 10^7\text{ N}\cdot\text{mm}/^\circ$, $k_{\theta_y}=4.5\times 10^7\text{ N}\cdot\text{mm}/^\circ$, $k_{\theta_z}=5.5\times 10^5\text{ N}\cdot\text{mm}/^\circ$,试验与仿真结果如表5。

表5 方位轴系刚度辨识
Table 5 Stiffness identification of azimuthal shafting

Mode shape	Swing left and right	Swing back and forth	Rotate around azimuth shafting
Working conditions		1	
Test/Hz	42.4	58	40.1
Simulation/Hz	43	58.4	39.2
Relative error/%	1.4	0.6	2.2

2.3.3 俯仰锁紧刚度辨识

工况2在工况1的基础上,俯仰锁紧机构处于锁紧状态,单独分析俯仰锁紧刚度。光电负载绕俯仰轴旋转、转台的前后摆动以及左右摆动均由俯仰锁紧刚度决定。即俯仰锁紧刚度参数 k_x 决定转台前后摆动阶振型固有频率; k_y 和 k_z 决定转台左右摆动阶振型固有频率; k_z 和 k_{θ_y} 决定载物台绕俯仰轴旋转阶振型固有频率。根据工况2的试验结果,试算确定 $k_x=50\ 000\text{ N}/\text{mm}$, $k_y=50\ 000\text{ N}/\text{mm}$, $k_z=30\ 000\text{ N}/\text{mm}$, $k_{\theta_y}=3\times 10^7\text{ N}\cdot\text{mm}/^\circ$, $k_{\theta_z}=3\times 10^7\text{ N}\cdot\text{mm}/^\circ$,试验与仿真结果如表6。

表6 俯仰锁紧刚度辨识
Table 6 Stiffness identification of pitching locking devices

Mode shape	Swing back and forth	Swing left and right	Rotate around pitching shafting
Working conditions		2	
Test/Hz	61.2	46.6	40.6
Simulation/Hz	61.8	46.3	41.4
Relative error/%	0.9	0.6	1.9

2.3.4 方位锁紧刚度辨识

工况3在工况2的基础上,方位锁紧机构处于锁紧状态,单独分析方位锁紧的刚度。4个方位锁紧相对方位轴成对称分布,相互约束,因而只具有位移刚度,假定每个方位锁紧对整体刚度的贡献相等,具有相同

的刚度矩阵。该工况中,转台前后摆动、左右摆动以及上下摆动均由方位锁紧刚度决定,即方位锁紧刚度参数 k_x 和 k_y 共同决定转台前后摆动阶和左右摆动阶振型固有频率; k_z 决定转台沿方位轴上下摆动阶振型固有频率。根据工况3的试验结果,试算确定 $k_x=15\ 000\ \text{N/mm}$, $k_y=15\ 000\ \text{N/mm}$, $k_z=25\ 000\ \text{N/mm}$,试验与仿真结果如表7。

表7 方位锁紧刚度辨识
Table 7 Stiffness identification of azimuth locking devices

Mode shape	Swing left and right	Swing back and forth	Swing up and down
Working conditions		3	
Test/Hz	67.4	66.5	186.5
Simulation/Hz	68.8	66.9	184.8
Relative error/%	2.0	0.6	0.9

通过理论计算及模型参数识别,最终得到各Bushing单元刚度矩阵如表8。

表8 各Bushing单元刚度
Table 8 The stiffness coefficient of each Bushing elements

	Stiffness					
	$k_x /$ ($\text{N}\cdot\text{mm}^{-1}$)	$k_y /$ ($\text{N}\cdot\text{mm}^{-1}$)	$k_z /$ ($\text{N}\cdot\text{mm}^{-1}$)	$k_{\theta x} /$ ($\text{N}\cdot\text{mm}/^\circ$)	$k_{\theta y} /$ ($\text{N}\cdot\text{mm}/^\circ$)	$k_{\theta z} /$ ($\text{N}\cdot\text{mm}/^\circ$)
Azimuth shafting	2.5×10^5	2.5×10^5	1.1×10^5	2.5×10^7	4.5×10^7	5.5×10^5
Left-pitching shafting	1.6×10^5	1.6×10^5	70 000	5.1×10^7	5.1×10^7	4×10^5
Right-pitching shafting	30 000	30 000	300	0	0	0
Pitching locking devices	50 000	50 000	30 000	0	3×10^7	3×10^7
Azimuth locking devices	15 000	15 000	25 000	0	0	0

分别采用Bushing单元对锁紧机构和轴系等效建模(仿真1),采用MPC单元对锁紧机构和轴系等效建模(仿真2),采用MPC单元对锁紧机构等效建模, Spring单元对轴系等效建模(仿真3),模态仿真及试验结果对比如表9。

表9 仿真与试验固有频率对比
Table 9 Comparison of nature frequency between simulation and modal test

Modal shape	Modal Test	Simulation 1	Simulation 2	Simulation 3
	Nature frequency/Hz			
Rotate around pitching shafting	44.1	44.7	43.4	34.7
Swing back and forth	66.5	67.9	85.1	73.4
Swing left and right	67.4	69.1	96.2	78.4
Rotate around azimuth shafting	106.7	110.1	135.4	127.8
Local modal	174.8	167.7	190.4	143.6
Swing up and down	186.5	184.4	368.9	201.9

对比上述仿真和试验结果可得:Bushing单元等效建模能准确反映结构动态特性,固有频率与振型匹配度高,如图11所示。仿真2中使用MPC单元等效锁紧机构和轴系,连接刚度过大,各阶固有频率均高于模态试验结果,尤其转台沿着方位轴上下摆动阶固有频率偏差过大,建模失真严重。相比于仿真2,仿真3中轴系采用Spring单元等效建模,各阶固有频率有一定降低,能在一定程度上反映结构动态特性,但仍与模态试验结果有较大偏差。

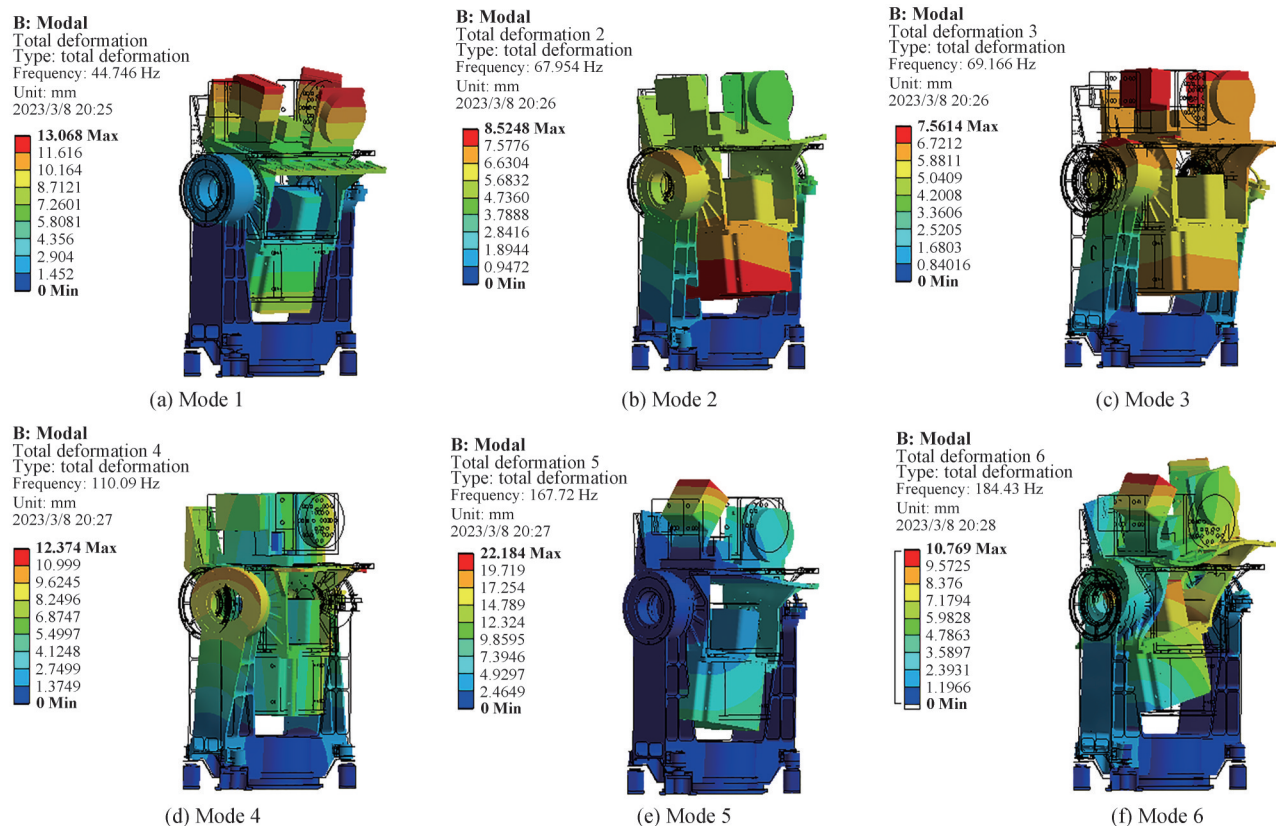


图 11 仿真分析前 6 阶振型图
Fig.11 The first six mode shapes by modal test

3 跟瞄转台阻尼特性分析

阻尼作为结构动态特性的基本参数,对固有频率影响很小,但会抑制共振频率处的响应幅值。有限元分析中常用的阻尼形式为恒定阻尼(Constant Damping),即每个频率对应的阻尼比都是恒定的,通常取 0.01~0.05,但在实际转台振动试验中,阻尼往往随频率非线性变化。直接模态阻尼(Modal Damping)是与频率相关的函数,通过定义对应于每阶振型的阻尼,抑制对应频段响应。由于阻尼效应是叠加的,在恒定阻尼比取 0.02 的基础上,通过扫频试验的数据对各阶模态阻尼进行辨识,分析跟瞄转台的阻尼特性。

带工装夹具的转台固定在振动台上,试验采用四点平均控制,即用安装在试验夹具上表面的四个传感器频响测量值的平均值控制振动台激励,8 个三向加速度传感器粘接在转台不同位置,输入条件如表 10,试验现场及测点如图 12 所示。

表 10 0.2 g 正弦扫频试验条件
Table 10 Test condition of 0.2 g swept-sine vibration test

Orientation	Frequency/Hz	Vibration level (g)	Tolerance
X, Y, Z	5~200	0.2(4 oct·min ⁻¹)	≤25 Hz, ±0.5 Hz
			>25 Hz, ±2%

扫频试验响应曲线如图 13 所示,与第 2 节中 Bushing 单元模型有限元分析结果对比如表 11,试验结果与仿真结果一致性良好,最大相对误差为 5.1%,在误差允许的范围,验证了连接部位刚度特性分析的准确性。

提取响应曲线中 X、Y、Z 三个主方向上的最大响应及其对应的共振频率,根据最大响应确定系统阻尼参数。取恒定阻尼比为 0.02,采样频率为 1 Hz,进行谐响应仿真分析,通过调整模态阻尼试算,使对应测点处的响应结果与试验结果匹配,得出 2 阶模态阻尼参数为 0.015,3 阶模态阻尼参数为 0.01,6 阶模态阻尼参数为 0.005。代入最终得出的阻尼参数,仿真与试验结果对比如表 12,试验响应曲线与仿真响应曲线对比如图 14 所示。

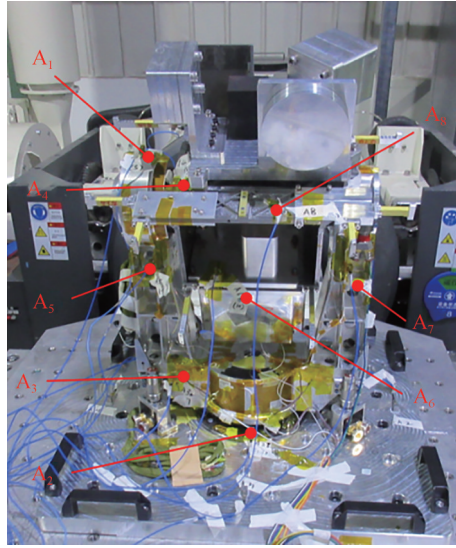


图 12 扫频试验测点图

Fig.12 Measurement points in swept-sine vibration test

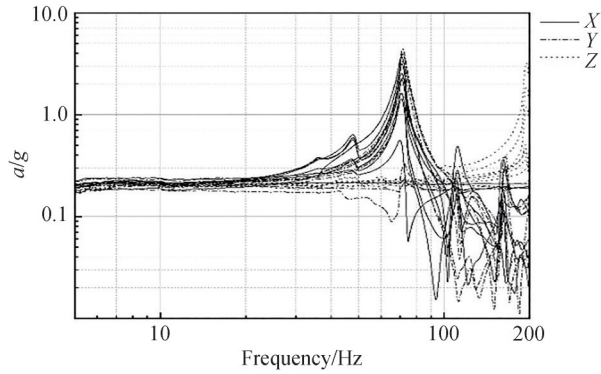


图 13 0.2 g 正弦扫频试验曲线

Fig.13 0.2 g swept-sine vibration test curve

表 11 0.2 g 扫频试验结果及仿真误差

Table 11 0.2 g swept-sine vibration test results and simulation errors

Mode	Test/Hz	Simulation/Hz	Relative error/%
1	47.1	44.7	5.3
2	69.9	67.9	2.8
3	71.2	69.1	2.9
4	111.3	110.1	1.1
5	165	167.7	1.6
6	193.2	184.4	4.6

表 12 模态阻尼系数辨识

Table 12 Modal damping coefficient identification

Orientation	MAX response point	Mode	Test response/g	Simulation response/g	Relative errors/%
X	A ₆	2	3.68	3.56	3.2
Y	A ₁	3	4.39	4.38	0.2
Z	A ₈	6	3.19	3.09	3.1

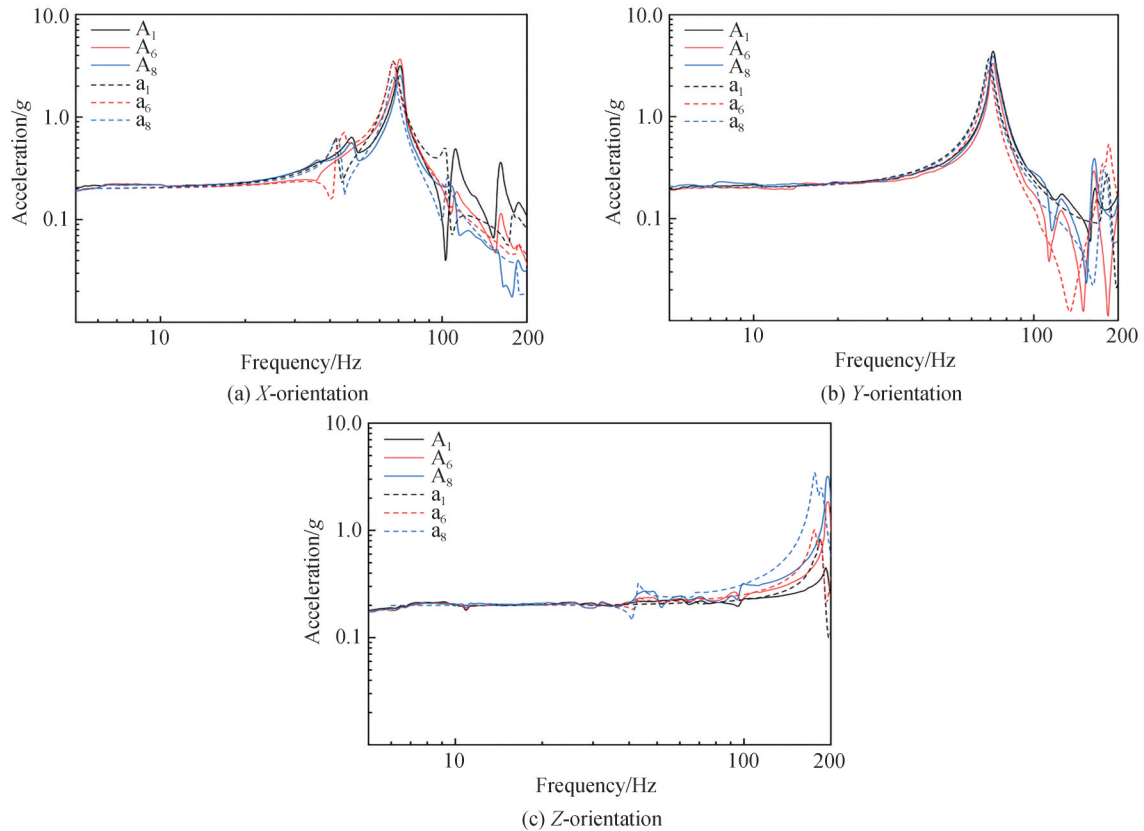


图14 试验与仿真响应曲线对比

Fig.14 The response curves comparison of test with simulation

图中 A_1 、 A_6 、 A_8 为三个测点的试验响应曲线, a_1 、 a_6 、 a_8 为三个测点的仿真响应曲线。仿真和试验曲线拟合度较高,三个主方向的最大响应匹配,最大相对误差为3.2%。

5 结论

本文根据某星载光电跟瞄转台的结构组成,建立整机等效有限元模型,对其动态特性进行了研究。使用广义弹簧单元(Bushing)对轴承和锁紧机构进行等效建模,通过理论计算和多工况模态试验数据确定了各连接部位刚度参数,有限元分析固有频率相对误差最大为5.1%,相比于传统建模方法能更准确反映转台刚度特性;通过0.2 g正弦扫频试验数据确定了系统模态阻尼,主方向最大响应相对误差最大为3.2%,均在允许的误差范围内,动态特性分析准确。

参考文献

- [1] CUI Kai. Study of the dynamics coupling between the two-axis gimbal and the satellite bus[D]. Beijing: University of Chinese Academy of Sciences, 2013.
崔凯. 二维跟踪转台与卫星平台的动力学耦合技术研究[D]. 北京: 中国科学院大学, 2013.
- [2] WANG Z C, HUANG M, QIAN L L, et al. Near-earth space two-dimension opto-electronic turntable design[J]. Optik, 2020, 200: 163387.
- [3] WANG Yaxiong, SHAO Yanan, WANG Pu. The design of Satellite-based small two-axis stabilized pointing turntable [J]. Equipment Manufacturing Technology, 2018(5):118-122.
王雅雄, 邵雅男, 王璞. 星载小型二轴稳瞄转台结构设计[J]. 装备制造技术, 2018(5): 118-122.
- [4] LI Zhaohui, CHEN Bo. Design and analysis of lunar-based tracking turntable for earth observation [J]. Acta Photonica Sinica, 2010, 39(12):2215-2219.
李朝辉, 陈波. 月基对地观测跟踪转台设计与分析[J]. 光子学报, 2010, 39(12): 2215-2219.
- [5] CHEN Zhuo, HU Qinglong, LI Zhaohui. Structural optimization of 2-D tracking turntable with carbon fiber framework for spatial target detection[J]. Optics and Precision Engineering, 2021, 29(3):547-557.

- 陈卓,胡庆龙,李朝辉.基于碳纤维框架天基目标探测二维跟踪转台结构优化[J].光学精密工程,2021,29(3):547-557.
- [6] GAO Duorui, XIE Zhuang, MA Rong, et al. Development current status and trend analysis of satellite laser communication (invited)[J]. Acta Photonica Sinica, 2021, 50(4): 0406001.
高铎瑞,谢壮,马榕,等.卫星激光通信发展现状与趋势分析(特邀)[J].光子学报,2021,50(4):0406001.
- [7] ZHENG Zhenzhen, ZHU Zhencai, KANG Yizhou. Overview of space-based optical observation systems for space debris and development of key technologies[J]. Acta Optica Sinica, 2022, 42(17): 189-196.
郑珍珍,朱振才,康一舟.天基空间碎片可见光观测系统与关键技术发展概述[J].光学学报,2022,42(17):189-196.
- [8] LV Yuehai. Research on the status quo of satellite optical communication[J]. Wireless Internet Technology, 2015(10): 27-28.
吕岳海.卫星光通信的现状研究[J].无线互联科技,2015(10):27-28.
- [9] WANG Zhi, LI Zhaohui. Design of optical-mechanical structure for lunar-based extreme ultraviolet camera[J]. Optics and Precision Engineering, 2011, 19(10): 2427-2433.
王智,李朝辉.月基极紫外相机光机结构设计[J].光学精密工程,2011,19(10):2427-2433.
- [10] ZHANG Yongqiang. Study on finite element modeling and stiffness characteristics of angular contact ball bearings [D]. Beijing: University of Chinese Academy of Sciences, 2017.
张永强.角接触球轴承刚度特性研究及其有限元建模分析[D].北京:中国科学院大学,2017.
- [11] HE Shuai, WANG Zhongsu. Modal analysis and experimental verification of two-dimensional turntable[J]. Manufacturing Automation, 2016, 38(5): 139-141, 146.
贺帅,王忠素.二维转台的模态分析与试验验证[J].制造业自动化,2016,38(5):139-141,146.
- [12] QING Tao, GUO Junli, ZHANG Meili, et al. Structure design and stiffness analysis of spaceborne two-dimensional turntable[J]. Infrared and Laser Engineering, 2022, 51(05): 300-308.
秦涛,郭骏立,张美丽,等.星载二维转台结构设计及刚度分析[J].红外与激光工程,2022,51(05):300-308.
- [13] CHEN Zhuo. Structural design and analysis for mechanical and thermal property of a spatial-based two-dimensional tracking and pointing mechanism[D]. Beijing: University of Chinese Academy of Sciences, 2015.
陈卓.一种天基二维跟踪指向机构的结构设计和力热特性分析[D].北京:中国科学院大学,2021.
- [14] ZHENG Shishan, ZHANG Liangyou, FU Ganwei. Modeling and simulation based on virtual prototype ADAMS for wire rope[J]. Mechanical Engineering & Automation, 2012(4): 26-28.
郑世山,张亮有,符敢为,等.基于虚拟样机ADAMS的钢丝绳建模及仿真[J].机械工程与自动化,2012(4):26-28.
- [15] XIAO Qi, Zhao Hailing, LU Shuai, et al. The dynamic analysis of tension stringing in transmission based on ADAMS [J]. Journal of Northeast Dianli University, 2016(6): 77-83.
肖琦,赵海玲,卢帅,等.以ADAMS为平台的张力架线动态仿真分析[J].东北电力大学学报,2016,36(6):77-83.
- [16] LIU Sheng. Design and deployment dynamic analysis for space double-layer pantograph antenna [D]. Xi'an: Xidian University, 2014.
刘升.空间双剪式铰天线设计与展开过程动力学分析[D].西安:西安电子科技大学,2014.
- [17] YAND Yanmeng, YAO Jianjun, YAN Hongsong, et al. Research on bearing dynamics modeling method of INS rotating mechanism[J]. Navigation Positioning and Timing, 2019, 6(3): 131-138.
杨研蒙,姚建军,闫红松,等.惯导系统旋转机构轴承动力学建模方法研究[J].导航定位与授时,2019,6(3):131-138.
- [18] HARRIS T A, KOTZALAS M N. Advanced concepts of bearing technology (rolling bearing analysis, fifth edition, book 2)[M]. LUO Jiwei, MA Wei, transl. Beijing: China Machine Press. 2009: 6-7.
哈里斯 T A, 克兹拉斯 M N, 轴承技术的高等概念(滚动轴承分析,原书第5版,卷2)[M]. 罗继伟,马伟,译.北京:机械工业出版社.2009:6-7.
- [19] WANG Fuchuan. Finite element modeling and dynamic analysis of typical joint structure of spacecraft[D]. Harbin: Harbin Institute of Technology, 2020.
王福川.航天器典型连接结构有限元建模及动力学分析[D].哈尔滨:哈尔滨工业大学,2020.
- [20] CHEN Xiaodong. Research on the key technology of shafting design of solar array drive assembly[D]. Beijing: University of Chinese Academy of Sciences, 2021.
陈晓东.太阳能电池阵驱动机构轴系设计关键技术研究[D].北京:中国科学院大学,2021.

Dynamic Characteristics Analysis of Space Electro-optical Tracking and Pointing Turntable

PENG Jiali^{1,2,3}, RUAN Ping^{1,3}, XIE Youjin^{1,3}, LI Zhiguo^{1,3}, WANG Jiahao^{1,2,3}, HAN Jingyu^{1,2,3}

(1 Xi'an Institute of Optics and Precision Mechanics, Chinese Academy of Sciences, Xi'an 710119, China)

(2 University of Chinese Academy of Sciences, Beijing 100049, China)

(3 Key Laboratory of Space Precision Measurement Technology, Chinese Academy of Sciences, Xi'an 710119, China)

Abstract: The space electro-optical tracking and pointing turntable is a kind of space photoelectric payload, which is used to realize the stability of the optical axis and the tracking of the target in the space environment. In the process of launching, the turntable must endure many harsh mechanical environments such as vibration and shock, therefore, its dynamic characteristics directly determine the reliability of the turntable. When we use finite element method to analyze the dynamic characteristics, a finite element model that can accurately reflect the stiffness and damping characteristics of the turntable is the key to the analysis. The stiffness of the connected parts in the turntable, such as bearings and locking devices, has a great influence on the stiffness characteristics of the overall structure. In the current research, there is a distortion problem in the finite element modeling of bearings and locking devices.

Aiming at this problem, this paper proposes an equivalent modeling method for bearing and locking devices by using generalized spring elements (bushing), which represents the behavior of a flexible connection or joint that allows translational and rotational movement. The translational degrees of freedom allow movement along the X , Y , and Z axes, representing the linear displacements in those directions, the rotational degrees of freedom allow rotation around the X , Y , and Z axes. We analyze the bearings and locking devices under dynamic load, establish their mechanical models, and define the significance of the Bushing elements stiffness matrix parameters. Then we simplify the structure of turntable, complete the equivalent modeling for shafting and locking devices by using Bushing elements, establish the finite element model of the turntable. Afterwards, we calculate a partial of bearing stiffness parameters based on Hertz contact theory. The remaining bearing stiffness parameters and all locking devices stiffness parameters that can not be theoretically calculated are obtained by parameter identification based on modal test data. Due to the stiffness of the bearings and locking devices decoupled from each other, we set up three different working conditions of modal test to obtain them. We use condition 1 (all locking devices: unlocked) to obtain the stiffness parameters of azimuth shafting and pitching shafting, condition 2 (azimuth locking devices: unlocked; pitching locking device: locked) to obtain the stiffness parameters of pitching locking device, and condition 3 (all locking devices: locked) to obtain the stiffness parameters of azimuth locking devices. Based on the obtained stiffness parameters, modal analysis is performed, the maximum relative error in natural frequencies between simulation and test is 5.1%, within the allowable margin. Finally, since the damping in the turntable system is a frequency-dependent damping, the constant damping used in traditional finite element analysis does not reflect real damping characteristics, we define damping characteristics of turntable by using modal damping. Modal damping is a frequency-dependent type of damping in finite element analysis, and suppresses responses by defining damping to each mode shape. Because of the superposition principle of damping effect, we use the maximum response of the X , Y , and Z directions in the 0.2 g swept-sine vibration test to identification the modal damping based on the constant damping of 0.02. Based on the obtained modal damping, harmonic response analysis is performed, the maximum relative error in the maximum responses of the X , Y , and Z directions between simulation and test is 3.2%, within the allowable margin. Hence the stiffness and damping parameters analysis of turntable is accurate, and the dynamic characteristics analysis is accurate.

The results show that the method of using Bushing elements to model the bearing and locking devices equivalently can reflect the dynamic characteristics of the turntable more accurately than traditional modeling methods, and the methods of obtaining the stiffness and damping characteristics through theoretical calculation and parameter identification are feasible. It has a certain reference effect on the modeling and simulation of the same type of turntable.

Key words: Precision instrument and machinery; Dynamic characteristic; Equivalent modeling; Space Electro-optical tracking and pointing turntable; Stiffness and damping; Natural frequency; Vibration response; Finite element analysis

OCIS Codes: 120.6085; 120.7280; 350.4600